A fast simulation method with arbitrary viscosity law

M. N. Macrossan

Centre for Hypersonics, School of Engineering, University of Queensland, St Lucia, 4072, Australia

Abstract. A new approach to DSMC collision modelling, called viscosity-DSMC or μ-DSMC, is described in which the time-averaged temperature is used to set the characteristic collision cross-section in each cell such that the Chapman-Enskog viscosity is that given by *any* desired viscosity law $\mu = \mu(T)$, including a curve fit to experimental data. For example, a hard sphere collision model, with hard sphere collision probability, used with a different molecular size in each cell can reproduce a Sutherland viscosity law. Similarly, a variable hard sphere collision model can reproduce the viscosity given by the more complicated generalized hard collision model, by making the reference cross-section a function of the temperature. This model is used to calculate the structure of a plane 1D shock and the results agree closely with those from standard DSMC using the GHS model. A particularly simple method is to use the Maxwell VHS model, in which all collision pairs are equally likely, to produce any desired viscosity law. The time-averaged cell temperature is available in standard DSMC as part of the procedures which determine the steady state flow and the new methods are as fast as, or faster than standard DSMC. Unlike more complicated models with realistic viscosities, the new procedures are compatible with the Borgnakke-Larsen energy exchange scheme and the established chemistry models for DSMC.

VISCOSITY OF REAL GASES AND THE VHS MODEL

The most commonly used DSMC collision model is the variable hard sphere (VHS) which gives rises to a power law viscosity $\mu \propto T^{\omega}$. Although this viscosity law is reasonably accurate over a limited range of temperature for a particular gas it does not represent a realistic viscosity over all temperatures. For $T < 2000$ K, the viscosity of a typical gas displays a significant deviation from a simple power law as a result of the long-range attractive forces between molecules. Fig. 1 shows the viscosity of argon compared with the two extremes of the power law, $\omega = \frac{1}{2}$, corresponding to hard spheres with constant cross-section, and $\omega = 1$ corresponding to a 'Maxwell molecule'. Also

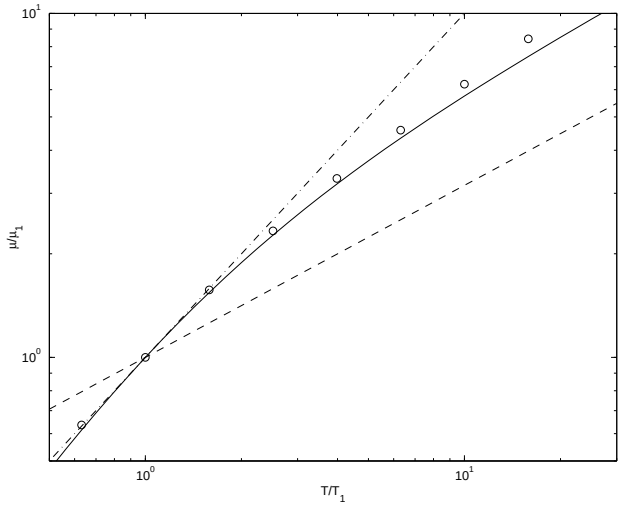

FIGURE 1. Viscosity for: —, Sutherland, Eq. 1; – –, hard sphere $\mu/\mu_1 = (T/T_1)^{\frac{1}{2}}$; · – ·, linear law $\mu/\mu_1 = T/T_1$. ∘ argon data Kestin *et al.* [1] $T_1 = T_s = 142$ K, $\mu_1 = 1.129 \times 10^{-5}$ Nm^{-1} s^{-1}.

CP762, *Rarefied Gas Dynamics: 24th International Symposium,* edited by M. Capitelli

Report Documentation Page

Form Approved
OMB No. 0704-0188

1. REPORT DATE	2. REPORT TYPE	3. DATES COVERED
13 JUL 2005	**N/A**	**-**

4. TITLE AND SUBTITLE	5a. CONTRACT NUMBER
A fast simulation method with arbitrary viscosity law	5b. GRANT NUMBER
	5c. PROGRAM ELEMENT NUMBER
6. AUTHOR(S)	5d. PROJECT NUMBER
	5e. TASK NUMBER
	5f. WORK UNIT NUMBER
7. PERFORMING ORGANIZATION NAME(S) AND ADDRESS(ES) **Centre for Hypersonics, School of Engineering, University of Queensland, St Lucia, 4072, Australia**	8. PERFORMING ORGANIZATION REPORT NUMBER
9. SPONSORING/MONITORING AGENCY NAME(S) AND ADDRESS(ES)	10. SPONSOR/MONITOR'S ACRONYM(S)
	11. SPONSOR/MONITOR'S REPORT NUMBER(S)

12. DISTRIBUTION/AVAILABILITY STATEMENT
Approved for public release, distribution unlimited

13. SUPPLEMENTARY NOTES
See also ADM001792, International Symposium on Rarefied Gas Dynamics (24th) Held in Monopoli (Bari), Italy on 10-16 July 2004.

14. ABSTRACT

15. SUBJECT TERMS

16. SECURITY CLASSIFICATION OF:			17. LIMITATION OF ABSTRACT	18. NUMBER OF PAGES	19a. NAME OF RESPONSIBLE PERSON
a. REPORT **unclassified**	b. ABSTRACT **unclassified**	c. THIS PAGE **unclassified**	**UU**	**6**	

shown is the Sutherland viscosity,

$$\mu/\mu_1 = (T/T_1)^{1/2}\,(1+T_s/T_1)/(1+T_s/T), \tag{1}$$

where $T_s = 142$ K and $\mu_1 = \mu(T_1)$ which fits the data better than any power law.

When using the VHS model in any particular DSMC calculation one can determine the range of temperatures expected in the flow and choose VHS parameters which match the viscosity reasonably well. However it would be better to have a collision model which fitted the experimental data over all temperatures. Realistic potentials, such as the Morse potential [2], the Lennard-Jones potential [3, 4] and the Maitland-Smith potential [5] have been used in DSMC as have other collision models [6, 7] which produce realistic viscosity laws, but these are not widely used. This is partly because of their relative complexity, but also because of the difficult of using the Borgnakke-Larsen energy exchange scheme [8] when the collision probability does not match that of the VHS collision model. The combination of the Borgnakke-Larsen (BL) exchange model and the VHS model is now the de facto standard of DSMC. Similarly, the DSMC procedures for chemically reacting flow [9] are built around the VHS model.

Here I show how an arbitrary viscosity law $\mu = \mu(T)$ can be realized in DSMC using simple collision models which are compatible with the BL exchange scheme. This is good not only in itself, but also because it makes the construction of hybrid DSMC/Navier-Stokes solvers easier; the viscosity law in both the DSMC and Navier-Stokes code can be the best available, rather than that dictated by computational practicality. The new method runs as fast, or faster than the standard VHS collision model.

The new method, called μ-DSMC, is to adjust the size of any simple collision model based on the local temperature to produce *any* desired viscosity at that temperature. We use the hard sphere and VHS collision models as the basis of the new method and in each case produce a viscosity law different from the usual one for that collision model. The method has been tested in Couette flow and for highly non-equilibrium flow in the interior of a shock and has been shown to produce essentially the same results as DSMC using more complicated collision models. A particular form of the general method, based on the Maxwell limit of VHS, is described and compared with standard DSMC in a zero-dimensional velocity relaxation calculation and the supersonic flow around a blunt-faced cylinder. In all cases the new method agrees well with standard DSMC; the deviations are small and confined to small regions of the flow. In all cases shown here a monatomic gas, with $\gamma = 5/3$ has been used.

HARD SPHERE MODEL WITH SUTHERLAND VISCOSITY

The Chapman-Enskog viscosity for hard spheres, with diameter d is

$$\mu = \frac{5m}{16}\frac{(\pi RT)^{1/2}}{\sigma},$$

where $\sigma = \pi d^2$ is the the total collision cross-section and $R = k/m$ is the ordinary gas constant. A given viscosity law $\mu = \mu(T)$ can be implemented by setting the cross-section in each cell as

$$\sigma(\bar{T}) = \frac{5m}{16}\frac{(\pi R\bar{T})^{1/2}}{\mu(\bar{T})}, \tag{2}$$

where $\bar{T}$ is the time-averaged translational kinetic temperature in the cell.

This method has been tested for supersonic Couette flow in Ref. [10], using the Sutherland viscosity (Eq. 1) for μ in Eq. 2. The measured shear stress $\tau_{\text{meas}} = \rho c_x c_y$, was determined from the steady-state velocity distribution and compared with the theoretical shear stress $\tau_t = \mu_{\text{suth}} du_x/dy$, where μ_{suth} is the Sutherland viscosity evaluated for the cell temperature. The ratio $\tau_{\text{meas}}/\tau_t$ in Fig. 2, is close to unity across most of the flow except in the Knudsen layer near the wall. The figure also shows that μ_{meas}/μ_t is significantly different from unity when μ_t is calculated using the hard sphere viscosity; in other words the hard sphere and Sutherland viscosities are significantly different for these temperatures. Thus, the hard sphere collision model with a different collision cross-section in each cell displays the Sutherland law as required.

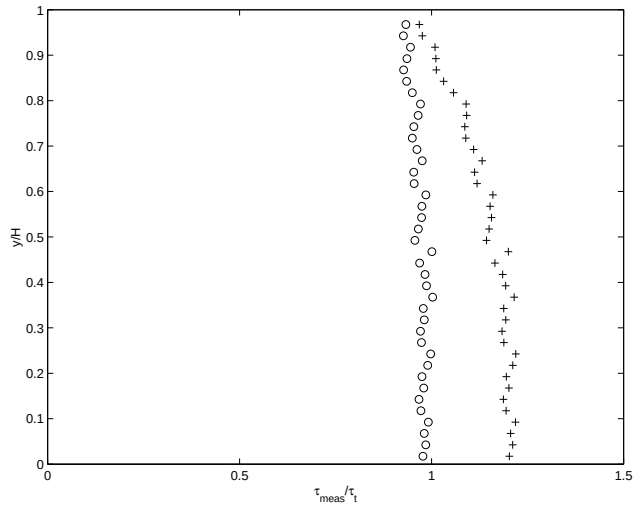

FIGURE 2. Measured shear stress in Couette flow simulation using μ-DSMC and Sutherland viscosity, compared with theoretical shear stress $\tau_t = \mu_t(T_{meas})\, du_x/dy_{meas}$. $\circ$, μ_t from Eq. 1 (Sutherland); $+$, $\mu_t = (T/T_1)^{1/2}$ (hard sphere). Origin of y-axis mid-way between the plates. Distance between plates $2H$. Nominal Knudsen number $2\mu_1/(\rho_1 \bar{c}_1 H) = 0.01$, $\bar{c} = (8RT_1/\pi)^{1/2}$, subscript 1 denotes undisturbed gas state. Wall temperature $T_w = T_1$. Wall speed $V_w = 3(2RT_1)^{1/2}$. Only 1 in 5 points shown. From Ref. [11].

VHS COLLISION MODEL WITH GHS VISCOSITY

The VHS collision model has a total collision cross-section given by

$$\sigma = \sigma_r (g_r/g)^{2\upsilon}$$

where g is the collision speed, σ_r is a reference cross-section, g_r is a constant reference speed and υ is a constant in the range 0 to $1/2$. With isotropic scattering and this total cross-section the theoretical viscosity is

$$\mu = \frac{15m}{8\Gamma(4-\upsilon)} \frac{(\pi RT)^{1/2}(4RT)^{\upsilon}}{\sigma_r g_r^{2\upsilon}} = \frac{15m}{8\Gamma(4-\upsilon)} \frac{(\pi RT)^{1/2}}{\sigma_r}$$

for $g_r = (4RT)^{1/2}$. To achieve an arbitrary viscosity law $\mu = \mu(T)$ the reference cross-section in each cell is set as

$$\sigma_r(\bar{T}) = \frac{15m}{8\Gamma(4-\upsilon)} \frac{(\pi R\bar{T})^{1/2}}{\mu(\bar{T})}.$$

In Ref. [10] this method, with $\upsilon = 1/6$ was used to calculate the structure of a plane normal shock, with the viscosity specified as that for the generalized hard sphere (GHS) [6]

$$\mu = \frac{15\pi^{1/2}}{16\Gamma(4-\upsilon_1)} \frac{(T/T_0)^{1/2+\upsilon_1}}{[\phi + (1-\phi)S]} \frac{mg_0}{\sigma_0}. \tag{3}$$

With $\phi = 0.61$, $\upsilon_1 = 2/13$, $\upsilon_2 = 14/13$, $\sigma_0 = 6.457 \times 10^{-19}\text{m}^2$, $T_0 = 300$ K, $S = S_0 (T_0/T)^{\upsilon_2 - \upsilon_1}$ and $g_0 = (4RT_0)^{1/2}$, Eq. 3 fits the data for argon better than the Sutherland law. The value of S_0 was set so that $\mu(300) = 2.272 \times 10\ \text{Nm}^{-1}$.

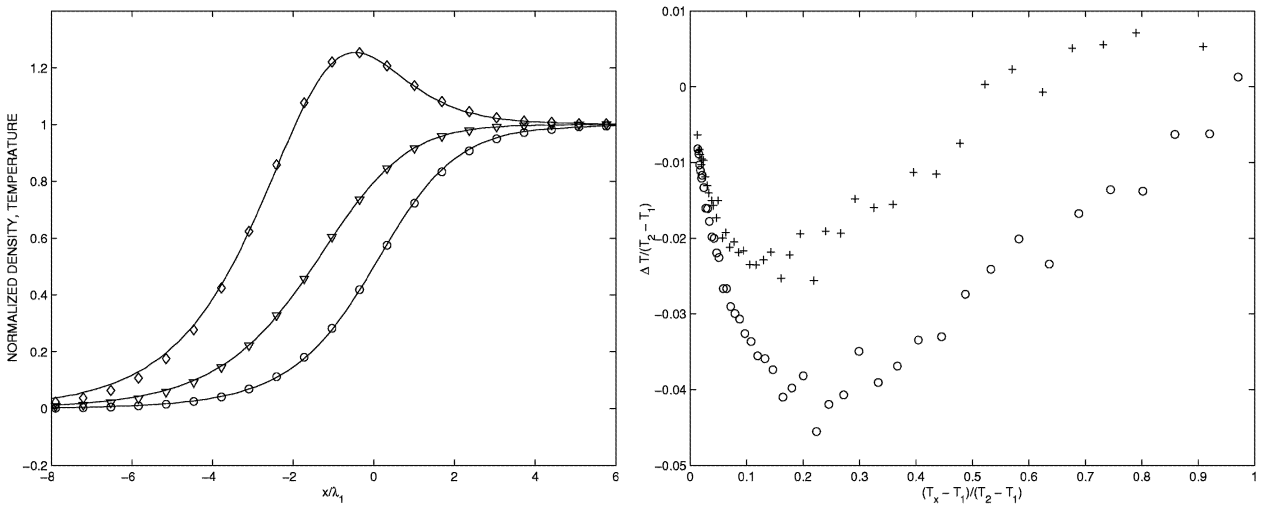

FIGURE 3. (a) Normalized density and temperature profiles for normal shock ($M_1 = 4$, $T_1 = 150$ K, $\gamma = 5/3$). Solid lines show DSMC (GHS) results; symbols are for modified μ-DSMC. $\diamond$, T_x; ∇, T_p; $\circ$, ρ. (b) Differences between T_x calculated by DSMC (GHS) and μ-DSMC for the shock in part (a). The 'error' is expressed as a percentage of the temperature jump across the shock. $\circ$, standard μ-DSMC, maximum error 4.6%; $+$, modified μ-DSMC, maximum error 2.6%. From Ref. [10]

The μ-DSMC results for a Mach 4 shock with this viscosity are compared in Fig. 3 with DSMC results using the GHS model[1] for which the total collision cross-section is given by

$$\sigma/\sigma_0 = \phi\,(g_0/g)^{2\upsilon_1} + (1-\phi)\,(g_0/g)^{2\upsilon_2}\,.$$

Fig. 3(a) shows the shock profiles of ρ, T_x and parallel temperature $T_p = (T_y + T_z)/2$ for both methods. The new method produces results almost identical to those for standard DSMC using the GHS collision model. There is a slight difference in the T_x profiles in a small region upstream of the shock. In the case shown a small modification was used for μ-DSMC; the size of collision cross-section was calculated from Eq. 3 using $\bar{T}_x$, rather than $\bar{T}$. Fig. 3(b) shows the differences in the T_x profiles, between DSMC and μ-DSMC, the latter using both $\bar{T}$ and $\bar{T}_x$. The maximum deviation from DSMC is 4.6% of the temperature rise across the shock for standard μ-DSMC and 2.6% for the modified method.

MAXWELL CROSS-SECTION WITH VISCOSITY $\propto T^{\omega}$

The 'Maxwell VHS' model [13] is the special case ($\upsilon = 1/2$) of the VHS model for which

$$\sigma = \sigma_r g_r / g.$$

The collision probability ($\propto g\sigma$) is independent of relative speed g for this model. The collision loops are particularly simple which can increase the computational speed. When the reference cross-section in each cell is adjusted according to the desired viscosity law, the collision rate and number of collisions required in one time step Δt become

$$\nu\,(\bar{T}) = 2\bar{n}k\bar{T}/\mu\,(\bar{T}) \quad \text{and} \quad N_{\text{coll}} = \bar{n}k\bar{T}/\bar{\mu} \times N\Delta t$$

respectively, where $\bar{n}$ is the time-averaged number density and N is the number of simulator particles in the cell. Note that the use of $\bar{n}$ is standard in DSMC [14] and that $\bar{T}/\mu\,(\bar{T})$ can be calculated at regular intervals for each cell.

This method was called 'collision rate DSMC' (ν-DSMC) in Ref. [11] where its behavior in a zero-dimensional

[1] A slight modification of the collision cross-section for $g < g_0$ was used which makes the GHS model computationally efficient, with negligible effect on its theoretical viscosity. See Refs. [12] and [10].

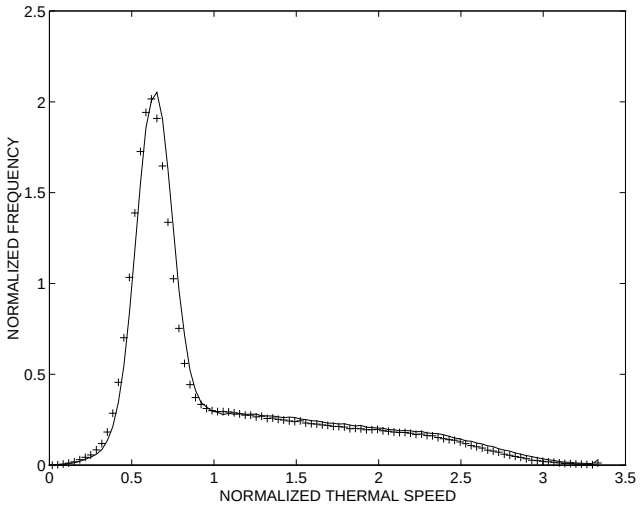

FIGURE 4. Thermal speed distribution after one nominal collision time $t = 2\mu/\left(\rho\bar{c}^2\right)$, where $\bar{c} = (8RT_e/\pi)^{1/2}$, is the mean thermal speed and T_e is the equilibrium (or kinetic) temperature. The initial distribution was bi-modal corresponding to a high speed, high temperature jet mixed with a low temperature gas at rest. —, DSMC (VHS) with $\upsilon = 0.31$; $+$, ν-DSMC with matching viscosity $\mu\left(T_e\right)$. The collision rate for ν-DSMC $\approx$ 21% greater than for DSMC (VHS). From Ref. [11]

relaxation calculation was compared with standard DSMC. Every DSMC calculation requires such a relaxation calculation in each cell at each time step. If, starting from any non-equilibrium distribution of velocities, two different collision models give the same (statistical) velocity distribution at the end of the collision phase then the two models will produce identical results when used in DSMC, regardless of how many collisions each model requires.

In Ref. [11], ν-DSMC was tested against DSMC for a number of highly non-equilibrium initial velocity distributions. An example is shown in Fig. 4. In the initial state 1/5 of the particles had velocities selected from an equilibrium distribution with a mean (20,0,0) and a characteristic thermal speed of 3 (arbitrary units). The remaining 4/5 had a mean velocity (0,0,0) and characteristic speed of 1. The thermal speed distributions for the two methods are virtually the same after the same elapsed time $t = 2\mu/\left(\rho\bar{c}^2\right)$, where $\bar{c} = (8RT/\pi)^{1/2}$ is the mean thermal speed. The collision rate for ν-DSMC was about 21% greater than for standard VHS; a larger number of collision is required in ν-DSMC because, with the standard VHS model, collision pairs are weighted towards higher relative velocities so that an average VHS collision is more 'efficient' in redistributing energy. This same effect can be shown for the Krook and Wu near-equilibrium exact solutions of the Boltzmann equation [15]; different differential collision cross-sections give identical results if their (integrated) viscosity cross-sections are matched.

Simulations using ν-DSMC and VHS, with the same viscosity law $\mu \propto T^{0.72}$ ($\upsilon = 0.22$), were performed for the Mach 10 flow around a blunt-ended cylinder with its blunt face normal to the freestream velocity. The nominal Knudsen number was $Kn_{D,\infty} = 2\mu_\infty/\left(\rho_\infty \bar{c}_\infty D\right)$ = 0.03, and the wall temperature ratio T_w/T_∞ was 0.26. Fig. 5(a) shows Mach number contours which are virtually indistinguishable, except for the slight difference ahead of the shock. The agreement in the expansion round the sharp corner is very close. Fig. 5(b) shows the near stagnation line profiles of density ρ and x-component of translation temperature T_x. The density rises through the shock and near the cold wall where the temperature falls. The steep rise of T_x in the shock, ahead of the density rise, can be seen. The ν-DSMC and DSMC results agree except for the small difference in T_x ahead of the shock which was also seen in the 1D shock profiles of Fig. 3.

DISCUSSION AND CONCLUSIONS

Although it has not been demonstrated here, it is clear that, since a standard VHS collision model is used in each cell, the new method is compatible with the Borgnakke-Larsen energy exchange scheme and with the standard chemistry models of DSMC, which are also based on the VHS model. The new method makes the VHS model display an arbitrary viscosity relationship by adjusting the number of collisions calculated in each cell, based on the cell temperature. There

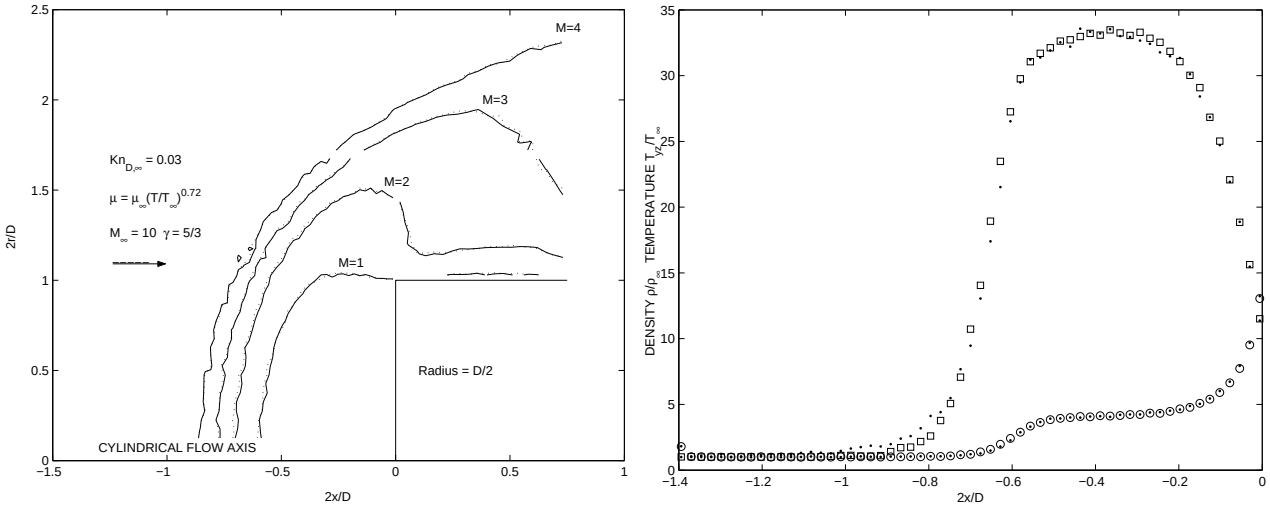

FIGURE 5. Antisymmetric flow about a blunt-faced cylinder. ν-DSMC compared with standard VHS model. $M_\infty = 10$, $T_w/T_\infty = 0.26$, $\gamma = 5/3$, $\mu/\mu_\infty = (T/T_\infty)^{0.72}$, $Kn_{D,\infty} = 2\mu_\infty/(\rho_\infty \bar{c}_\infty D) = 0.03$. (a) Mach number contours: – –, VHS; —-, ν-DSMC. (b) Temperature T_x and density ρ in cells adjacent to the stagnation streamline. □, VHS; •, ν-DSMC.

is virtually no extra computational overhead involved in obtaining the time-averaged temperature which is available in DSMC codes as the evolution of the flow is tracked to steady state. Although the cell temperature is not routinely used in DSMC as part of the simulation procedure, Bird has suggested [14] that it could be used to vary the exchange factor in the BL exchange scheme to agree with experimental results.

Any value of υ in the VHS model can be used as the basis of μ-DSMC. For $\upsilon = 0$ (hard sphere) the number of collisions calculated at each step is as low as possible, while for $\upsilon = 1/2$ (Maxwell VHS) the collision-pair selection is the easiest and the new method can be twice as fast as DSMC, although this depends on details of the code and flow. For the sake of a more realistic distribution of relative velocities in collisions an intermediate value of $\upsilon = 1/4$ might be better than either of the extreme values.

The new method has been shown to be accurate for the highly non-equilibrium flow in the interior of a shock and for the high speed flow around a blunt cylinder which contains an expansion around the sharp corner of the front face. Although more testing is desirable, the new method appears to be very promising.

REFERENCES

1. Kestin, J., Knierim, K., Mason, E. A., Najafi, B., Ro, S. T., and Waldman, M., *J. Phys. Chem. Ref. Data*, **13**, 229–303 (1984).
2. Davis, J., Dominy, R. G., Harvey, J. K., and Macrossan, M. N., *J. Fluid Mech.*, **135**, 355–371 (1983).
3. Sturtevant, B., and Steinhilper, E. A., "Intermolecular potentials from shock structure experiments," in *Rarefied Gas Dynamics. Proc. 8th Int. Symp.*, edited by Karamcheti, Acadmeic Press, 1974, p. 159.
4. Koura, K., and Matsumoto, H., *Phys. Fluids A*, **3**, 2459 – 2465 (1991).
5. Erwin, D. A., Pham-Van-Diep, G. C., and Muntz, E. P., *Phys. Fluids A*, **3**, 697 – 705 (1991).
6. Hash, D. B., and Hassan, H. A., *Phys. Fluids A*, **5**, 738 – 744 (1993).
7. Koura, K., and Matsumoto, H., *Phys. Fluids A*, **4**, 1083 – 1085 (1992).
8. Borgnakke, C., and Larsen, P. S., *J. Comput. Phys.*, **18**, 405 (1975).
9. Bird, G. A., *J. Comput. Phys.*, **25**, 353 (1977).
10. Macrossan, M. N., *J. Comput. Phys.*, **185**, 612–627 (2003).
11. Macrossan, M. N., *J. Comput. Phys.*, **173**, 600–619 (2001).
12. Macrossan, M. N., and Lilley, C. R., *J. Thermophys. Heat Trans.*, **17**, 289–291 (2003).
13. Erofeev, A. I., and Perepukhov, V. A., "Hypersonic rarefied flow about a flat plate by the Direct Simulation Method," in *Rarefied Gas Dynamics*, edited by Camprague, C.E.A, Paris, France, 1979, p. 417.
14. Bird, G. A., *Molecular Gas Dynamics and the Direct Simulation of Gas Flows*, Clarendon, Oxford, 1994.
15. Krook, M., and Wu, T. T., *Phys. Fluids*, **20**, 1589 – 1595 (1977).